

# Beneficial Role of Cetyltrimethylammonium Bromide in the Enhancement of Photovoltaic Properties of Dye-Sensitized Rutile TiO<sub>2</sub> Solar Cells

Hyun-Yong Byun,<sup>†</sup> R. Vittal,<sup>‡</sup> Dong Young Kim,<sup>§</sup> and Kang-Jin Kim<sup>\*†</sup>

*Division of Chemistry and Molecular Engineering, Korea University, Seoul 136-701, Korea, Central Electrochemical Research Institute, Karaikudi 630 006, India, and Polymer Materials Laboratory, Korea Institute of Science and Technology, Seoul 130-650, Korea*

*Received February 23, 2004. In Final Form: May 25, 2004*

A new approach involving the introduction of the common cationic surfactant cetyltrimethylammonium bromide (CTAB) for modifying a rutile TiO<sub>2</sub> film during its formation from hydrolyzed TiCl<sub>4</sub> solution has been adopted, intending to improve the photoelectrochemical properties of the pertinent dye-sensitized solar cell. CTAB-routed films were found to consist of smaller clusters of near-spherical TiO<sub>2</sub> particles, compared with larger clusters of long rod-shaped particles in the absence of CTAB. As a consequence, the photocurrent and photovoltage of the cell fabricated by using CTAB have increased significantly, leading to a conversion efficiency increase, compared with those of the cell prepared without CTAB. On the basis of FE-SEM, BET, and XRD analyses, the increases are attributed to decreased particle size, improved interparticle connectivity, and enhanced crystallinity of the CTAB-promoted TiO<sub>2</sub> particles and decreased void volume in the film. Faster growth of the TiO<sub>2</sub> film was another beneficial effect of CTAB. A mechanism is proposed for the beneficial role of CTAB during the film formation.

## Introduction

Dye-sensitized nanocrystalline TiO<sub>2</sub> solar cells (DSSCs) have been the subject of intense research in the past decade, as the best of these devices produced to date<sup>1</sup> is not efficient and cost-effective enough for converting solar energy into electricity. Altering the morphology and structure of the TiO<sub>2</sub> film and the size of TiO<sub>2</sub> particles and thereby the TiO<sub>2</sub> film electrode is one of the strategies for improving the efficiency of the cell.<sup>2–5</sup> For a nanocrystalline TiO<sub>2</sub> film, anatase has been widely regarded as the material of choice. Surprisingly, however, the photovoltages of anatase and rutile DSSCs are comparable at one-sun intensity.<sup>6,7</sup> Furthermore, compared with anatase, rutile TiO<sub>2</sub> has superior light scattering properties, because of its higher refractive index, and is chemically more stable and potentially cheaper to produce.<sup>8</sup> Higher light scattering properties are beneficial from the perspective of effective light harvesting. Hydrolysis of TiCl<sub>4</sub> is the process commonly used for obtaining highly porous rutile TiO<sub>2</sub> films for DSSCs.<sup>6,8</sup> However, analyses by intensity-modulated photocurrent spectroscopy along with SEM data suggest that electron transport is slower in the rutile layer than in the anatase layer due to differences

in interparticle connectivity associated with particle packing density.<sup>6</sup> Therefore, more densely packed films of smaller rutile TiO<sub>2</sub> nanoparticles are expected to improve the photocurrent. One possible way of achieving this goal is to utilize surfactants.

Surfactants have been used to produce a variety of TiO<sub>2</sub> materials. The first synthesis of a thermally stable hexagonally packed mesoporous TiO<sub>2</sub> by a modified sol-gel method, using an alkyl phosphate surfactant, was announced by Antonelli and Ying in 1995.<sup>9</sup> Putnam et al. have concluded that the hexagonal material exists, if at all, only as a minor component of a larger lamellar structure when phosphate surfactants are used.<sup>10</sup> Attempts have been made to use mostly nontypical surfactants as templates<sup>11</sup> in the formation of a TiO<sub>2</sub> film. Kobayashi and collaborators prepared a fibrous TiO<sub>2</sub> material with a “macaroni”-like structure by using their designed amphiphilic compound containing cationic charge moieties.<sup>12</sup> Kavan et al. used a polymeric surfactant, poly(alkylene oxide) block copolymer, as templating agent for the formation of anatase TiO<sub>2</sub> and investigated essentially Li<sup>+</sup> insertion.<sup>13</sup> Li and Tripp made an interesting study on the spectroscopic identification of aggregated structures of CTAB and the dynamics of their formation on TiO<sub>2</sub> surfaces.<sup>14</sup> Yang and co-workers used amphiphilic poly(alkylene oxide) block copolymers as structure-directing agents in nonaqueous solutions for organizing the network-forming metal oxide species that include TiO<sub>2</sub>.<sup>15</sup> Dobson and coresearchers deposited a TiO<sub>2</sub> film on a single internal

\* To whom correspondence should be addressed.

<sup>†</sup> Korea University.

<sup>‡</sup> Central Electrochemical Research Institute.

<sup>§</sup> Korea Institute of Science and Technology.

(1) O'Regan, B.; Grätzel, M. *Nature* **1991**, *353*, 737.

(2) Kavan, L.; Grätzel, M.; Rathouský, J.; Zúkal, A. *J. Electrochem. Soc.* **1996**, *143*, 394.

(3) Jung, K.-H.; Hong, J. S.; Vittal, R.; Kim, K.-J. *Chem. Lett.* **2002**, *864*.

(4) Papageorgiou, N.; Barbé, C.; Grätzel, M. *J. Phys. Chem. B* **1998**, *102*, 4156.

(5) Barbé, C. J.; Arendse, F.; Comte, P.; Jirousek, M.; Lenzmann, F.; Shklover, V.; Grätzel, M. *J. Am. Ceram. Soc.* **1997**, *80*, 3157.

(6) Park, N.-G.; van de Lagemaat, J.; Frank, A. J. *J. Phys. Chem. B* **2000**, *104*, 8989.

(7) Park, N.-G.; Schlichthörl, G.; van de Lagemaat, J.; Cheong, H. M.; Mascarenhas, A.; Frank, A. J. *J. Phys. Chem. B* **1999**, *103*, 3308.

(8) Kim, K.-J.; Benkstein, K. D.; van de Lagemaat, J.; Frank, A. J. *Chem. Mater.* **2002**, *14*, 1042.

(9) Antonelli, D. M.; Ying, J. Y. *Angew. Chem., Int. Ed. Engl.* **1995**, *34*, 2014.

(10) Putnam, R. L.; Nakagawa, N.; McGrath, K. M.; Yao, N.; Aksay, I. A.; Gruner, S. M.; Navrotsky, A. *Chem. Mater.* **1997**, *9*, 2690.

(11) Yang, P.; Zhao, D.; Margolese, D. I.; Chmelka, B. F.; Stucky, G. *Chem. Mater.* **1999**, *11*, 2813.

(12) Kobayashi, S.; Hanabusa, K.; Hamasaki, N.; Kimura, M.; Shirai, H. *Chem. Mater.* **2000**, *12*, 1523.

(13) Kavan, L.; Rathouský, J.; Grätzel, M.; Shklover, V.; Zúkal, A. *J. Phys. Chem. B* **2000**, *104*, 12012.

(14) Li, H.; Tripp, C. P. *Langmuir* **2002**, *18*, 9441.

(15) Yang, P.; Zhao, D.; Margolese, D. I.; Chmelka, B. F.; Stucky, G. *Nature* **1998**, *396*, 152.

reflection ZnSe prism and then CTAB on the film and studied its adsorption.<sup>16</sup> Jadhav synthesized TiO<sub>2</sub> nanoparticle mesoporous films from reverse micelles, using titanium(IV) isopropoxide, Triton X-100, AOT, cyclohexane, and Millipore water.<sup>17</sup> Favoriti et al. studied the coadsorption of naphthalene derivatives and CTAB on a titanium dioxide/water interface among other interfaces.<sup>18</sup> Elder and coworkers prepared and characterized zirconia-stabilized 25 Å TiO<sub>2</sub> anatase crystallites in a mesoporous structure templated by cetyltrimethylammonium chloride.<sup>19</sup>

As can be seen from the above references, and to the best of our knowledge, no attempt has been made to use conventional surfactants, such as CTAB, SDS, and Triton X 100, to improve the morphology, crystallinity, and particle size of rutile TiO<sub>2</sub>, intending in turn to improve the DSSC photovoltaics. This being the situation, we have chosen the most typical surfactants, the cationic CTAB, the anionic sodium dodecyl sulfate (SDS), and the nonionic Triton X-100, to study their influences on the rutile TiO<sub>2</sub> film formation on fluorine-doped tin oxide (SnO<sub>2</sub>:F) conducting glass, aiming at improving the morphology of the rutile TiO<sub>2</sub> film, which in turn can fulfill the requirements of a DSSC for obtaining higher cell efficiency. We also intended to decrease the crystal size of rutile TiO<sub>2</sub> particles in the film, which would lead to a higher surface area of the TiO<sub>2</sub> film and thereby higher dye adsorption. The basis for this specific surfactant approach has been the success of one of the authors in obtaining unailing beneficial effects of CTAB for the deposition of metal hexacyanoferrates in general<sup>20–22</sup> and CoO and NiO in particular.<sup>23</sup>

In this paper we describe the beneficial role of CTAB in the modification of a TiO<sub>2</sub> film on SnO<sub>2</sub>:F, and consequently the enhancement of the photovoltage and photocurrent of DSSCs. A possible mechanism is proposed for the beneficial role of CTAB in the film formation.

### Experimental Section

Titanium tetrachloride was used as the starting material to prepare a TiO<sub>2</sub> film by precipitation. TiCl<sub>4</sub> was added in drops to chilled water (ca 4 °C) to produce a concentration of 2 M. This was used as a stock solution for further experimentation. SnO<sub>2</sub>:F conducting glass plates (1.5 × 1.5 cm) (Libbey-Owens-Ford, TEC 8, 75% transmittance in the visible) were first cleaned with water and ethanol. Keeping them in a slanting position, two to three drops of an ethanolic solution of titanium(IV) butoxide (7% v/v) were allowed to flow freely on them. The treatment with titanium(IV) butoxide/ethanol solution was done to produce a thin layer of TiO<sub>2</sub> to isolate the conducting glass surface from the redox electrolyte.<sup>24</sup> The plates were then annealed at 450 °C for 30 min, cooled, and placed in different Petri dishes (60 × 15 mm), with the conducting side facing upward. Aliquots (10 mL) of 0.2 M TiCl<sub>4</sub> were pipetted out into these vessels, followed by the addition of 10 mL aqueous solutions of surfactants at different concentrations, as mentioned at appropriate places. All chemicals

were of analytical grade and used without further purification. All solutions were prepared using Milli-Q (18.2 MΩ) H<sub>2</sub>O. The closed vessels were set aside for 36–72 h at room temperature (22 °C) for the deposition of TiO<sub>2</sub>. Afterward, the deposited glass plates were rinsed with distilled water, dried for 10 min in an oven at 100 °C, and annealed at 450 °C for 1 h. Subsequently, their film thickness was measured with a Tencor alpha-step 250 profiler.

TiO<sub>2</sub> films thus obtained were coated with 0.3 mM [RuL<sub>2</sub>(NCS)<sub>2</sub>]·2H<sub>2</sub>O (where L = 2,2'-bipyridine-4,4'-dicarboxylic acid) in absolute ethanol for 12 h at room temperature. To minimize hydration of TiO<sub>2</sub> from moisture in the ambient air, the films were immersed in the dye solution while they were at around 100–120 °C after the annealing step. To prepare the counter electrode, 5 × 10<sup>-3</sup> M hexachloroplatinic acid in 2-propanol was spread on SnO<sub>2</sub>:F glass; the glass was then heated at 450 °C for 30 min. The platinum electrode was placed over the dye-coated TiO<sub>2</sub> electrode, and the edges of the cell were sealed with 1 mm wide strips of 25 μm thick Surlyn (Solaronix SA, SX1170 Hot Melt). A hot press was used to press together the film electrode and the counter electrode. The redox electrolyte consisted of 0.05 M I<sub>2</sub>, 0.1 M LiI, 0.7 M 1,2-dimethyl-3-hexylimidazolium iodide, and 0.5 M 4-*tert*-butylpyridine in 3-methoxypropionitrile. A drop of the electrolyte solution was introduced into the clamped electrodes through one of two small holes drilled in the counter electrode. The holes were then covered and sealed with small squares of Surlyn strip and microscope objective glass. The resulting cell had an active area of 0.4 × 0.4 cm. Photocurrent–voltage (*J*–*V*) curves were obtained using a Keithley M 236 source measure unit. A 300 W Xe arc lamp (Oriel) through an AM 1.5 solar simulating filter for spectral correction was used to illuminate the working electrode, and its light intensity was adjusted to be approximately 100 mW/cm<sup>2</sup>, using a Si solar cell. Incident photon-to-current conversion efficiency (IPCE) was measured with an Amino-Bowman fA-256 luminescence spectrometer. An HP 8453A diode array spectrophotometer was used for obtaining absorption spectra. Raman spectra were obtained using a Jasco NR1100 Raman spectrophotometer. The surface morphology and thickness of the films were obtained with field emission scanning electron microscopy (FE-SEM) using a Hitachi S-4300 microscope. XRD measurements were carried out using a MAC Science Co. MO3XHF X-ray diffractometer with Cu Kα radiation. The surface area was measured with the BET method (Micromeritics, ASAP 2010).

### Results and Discussion

A pronounced favorable influence of CTAB was observed on the morphology, crystallinity, and particle size of the TiO<sub>2</sub> film, leading to a great improvement in the photocurrent and photovoltage of DSSCs, which is evidenced in the discussion that follows. Different CTAB concentrations of 3 orders of magnitude, 9.2 × 10<sup>-4</sup> (its cmc), 1.0 × 10<sup>-2</sup>, and 0.92 M, were tested, keeping the TiCl<sub>4</sub> concentration at 0.2 M. Though at all concentrations CTAB proved itself to be useful in greatly improving the film properties from the perspective of solar conversion efficiency, its optimum beneficial influences were found at 1.0 × 10<sup>-2</sup> M. Hereafter, we restrict all our results with reference to this CTAB concentration, unless otherwise specified. Contrarily, anionic and nonionic surfactants did not show pronounced beneficial influence on film formation at 0.10 and 0.010 M SDS and Triton X-100, and at their cmc's of 8.3 × 10<sup>-3</sup> and 3.3 × 10<sup>-4</sup> M, respectively, although the film thickness and crystallinity of the particles decreased in both cases, compared with those without surfactant. In the case of SDS, the TiO<sub>2</sub> cluster size decreased slightly at 1.0 × 10<sup>-2</sup> M, compared with that obtained without SDS (cluster size 380–400 nm with SDS and 400–450 nm without SDS), which can be regarded as a favorable influence by the surfactant. No change in cluster size was observed at either 0.1 or 8.3 × 10<sup>-3</sup> M SDS. There was no change in the cluster size with Triton

(16) Dobson, K. D.; Roddick-Lanzilotta, A. D.; McQuillan, A. J. *Vib. Spectrosc.* **2000**, *24*, 287.

(17) Jadhav, A. V. *TiO<sub>2</sub> Nanoparticles as Photocatalysts*; Department of Material Science and Engineering, University of Cincinnati: Cincinnati, OH, pp 1–9.

(18) Favoriti, P.; Monticone, V.; Treiner, C. *J. Colloid Interface Sci.* **1996**, *179*, 173.

(19) Kavan, L.; Attia, A.; Lenzmann, F.; Elder, S. H.; Grätzel, M. *J. Electrochem. Soc.* **2000**, *147*, 2897.

(20) Vittal, R.; Jayalakshmi, M.; Gomathi, H.; Prabhakara Rao, G. *J. Electrochem. Soc.* **1999**, *146*, 786.

(21) Vittal, R.; Gomathi, H.; Prabhakara Rao, G. *Electrochim. Acta* **2000**, *45*, 2083.

(22) Vittal, R.; Gomathi, H. *J. Phys. Chem. B* **2002**, *106*, 10135.

(23) Vittal, R.; Gomathi, H.; Prabhakara Rao, G. *J. Electroanal. Chem.* **2001**, *497*, 47.

(24) Smestad, G. *Sol. Energy Mater. Sol. Cells* **1994**, *32*, 273.

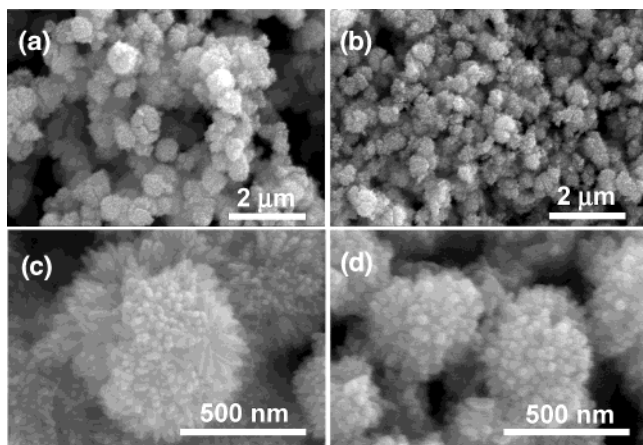


**Figure 1.** Plane-view FE-SEM images of a rutile TiO<sub>2</sub> film prepared from hydrolyzed TiCl<sub>4</sub> (a, c) without and (b, d) with CTAB.

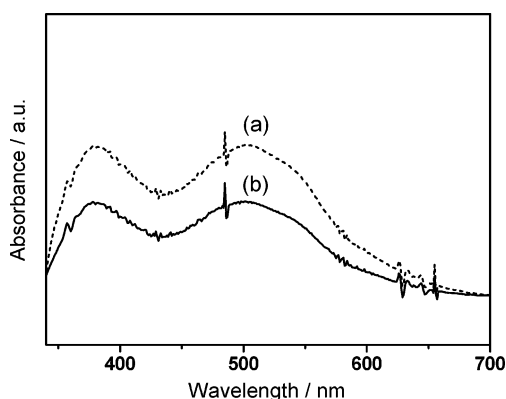


**Figure 2.** Absorption spectra of dye desorbed from (a) CTAB-influenced TiO<sub>2</sub> and (b) TiO<sub>2</sub> electrodes in  $1.0 \times 10^{-3}$  M KOH solution for 24 h.

X-100 at  $3.0 \times 10^{-4}$ ,  $1.0 \times 10^{-2}$ , or 0.10 M, compared with that without it.

Figure 1 compares plane-view SEM images of TiO<sub>2</sub> films prepared in the absence of CTAB (Figure 1a,c) and in the presence of CTAB (Figure 1b,d). Both films display highly porous structures, creating large void volumes in the film.<sup>8</sup> However, it can easily be seen that the film formed in the presence of CTAB is more densely packed due to smaller clusters consisting of near-spherical particles, compared with larger clusters with long rod-shaped particles formed without CTAB, suggesting an increase in the effective surface area of the former film. Indeed, BET surface area values were 35 and 41 m<sup>2</sup>/g for the particles formed without and with CTAB, respectively, representing an increase of more than 17% in the latter case. This is further evident by the observation that the amount of dye, desorbed from the CTAB-influenced film surface, has increased by 35% over that from the film formed without CTAB, as can be seen from the absorption spectra of dye desorbed from TiO<sub>2</sub> and CTAB-influenced TiO<sub>2</sub> electrodes in  $1.0 \times 10^{-3}$  M KOH solution for 24 h (Figure 2). Further, a more densely packed film is expected to lead to improved interparticle electrical contact. XRD analysis of the films in Figure 3 suggests that the average crystallite size in the film formed in the presence of CTAB is smaller than that formed in the absence of CTAB, according to the Scherrer equation on the basis of the broader line width in the former film. The rutile phase was confirmed by the XRD patterns. Furthermore, the increased XRD peak intensity indicates the enhanced crystallinity of the TiO<sub>2</sub> particles formed in the presence of CTAB. The additional

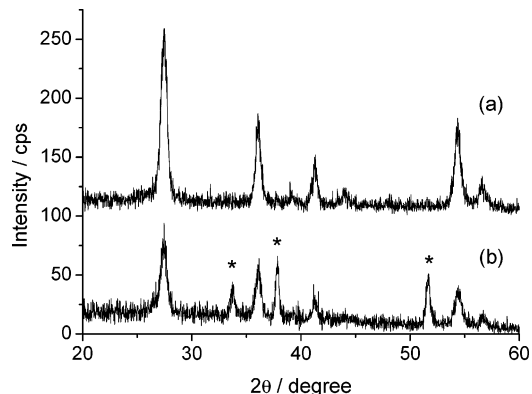


**Figure 3.** XRD patterns of rutile TiO<sub>2</sub> films formed (a) with and (b) without CTAB. The asterisks denote peaks attributed to FTO substrate.

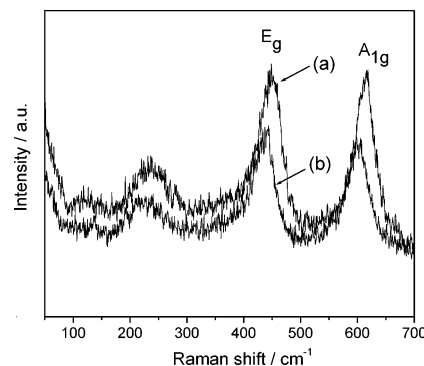


**Figure 4.** Raman spectra of rutile TiO<sub>2</sub> films formed (a) with and (b) without CTAB.

peaks marked by asterisks in Figure 3b at about 34°, 38°, and 52° are due to the substrate FTO under our experimental conditions. Absence of these peaks in the case of the film formed in the presence of CTAB (Figure 3a) is due to the densely packed nature of the film, covering the FTO surface completely, which would impede the penetration of X-rays deep into the film up to the FTO substrate. Xu and co-workers had prepared nanosized TiO<sub>2</sub> particles which were coated with the surfactants dodecylbenzenesulfonic acid and stearic acid using a hydrothermal procedure and obtained surfactant/TiO<sub>2</sub> particles that were 1 order smaller than those obtained in the absence of the surfactants under the same conditions.<sup>25</sup> Their results are consistent with the particle size reduction observed here using CTAB.

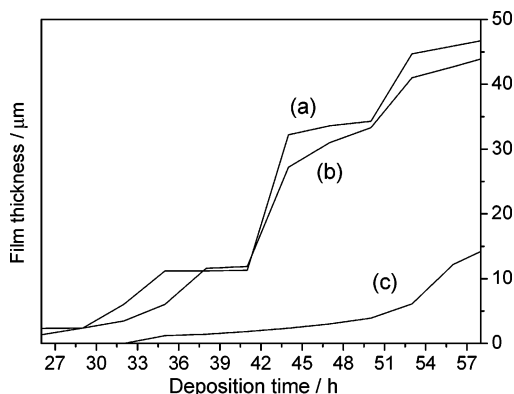
Figure 4 shows the CTAB influence on the Raman spectra of TiO<sub>2</sub> films. In both cases the crystal phase of the particles is also rutile, as can be judged from the bands at 612, 447, 232, and 142 cm<sup>-1</sup>.<sup>26,27</sup> A close observation of the bands at about 447 and 612 cm<sup>-1</sup> reveals that they are broadened and shifted to higher energy by about 13 cm<sup>-1</sup> in the case of the film formed with CTAB, relative to those obtained without CTAB. The decrease in the particle dimension of nanometer scale can cause a blue shift and broadening of the Raman peaks as a result of phonon confinement,<sup>25</sup> which is consistent with the XRD data mentioned above.

Figure 5 shows the deposition-time-dependent TiO<sub>2</sub> film thickness, indicating extremely fast film deposition in the

(25) Xu, C. Y.; Zhang, P. X.; Yan, L. *J. Raman Spectrosc.* **2001**, *32*, 862.

(26) Porto, P. S.; Fleury, P. A.; Damen, T. C. *Phys. Rev.* **1967**, *154*, 522.

(27) Felske, A.; Plieth, W. J. *Electrochim. Acta* **1989**, *34*, 75.



**Figure 5.** Thickness of a rutile TiO<sub>2</sub> film formed with (a) 0.1 M, (b) 0.01 M, and (c) 0.0 M CTAB as a function of deposition time.

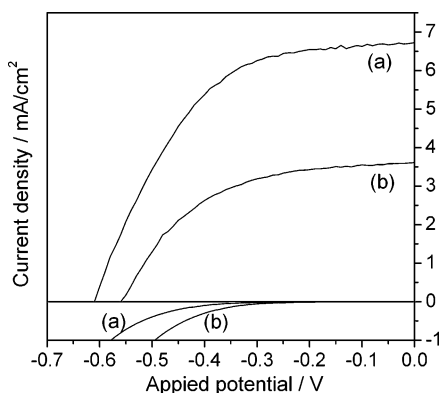


**Figure 6.**  $J$ - $V$  curves and dark currents of DSSCs prepared from hydrolyzed TiCl<sub>4</sub> (a) with and (b) without CTAB.

presence of CTAB, which is tantamount to pronounced thicker films at each point of time compared with the case without CTAB. For example, a film of about 12 μm thickness, which is generally regarded as the optimum thickness for a DSSC, is obtainable in about 37 h with 0.01 M CTAB, compared with nearly 57 h without CTAB. At 0.1 M CTAB, the film deposition rate is somewhat higher than that at 0.01 M CTAB. It should be mentioned here that the subsequent results are with reference to films of approximately 12 μm thicknesses, regardless of whether CTAB is used.

Figure 6 shows the striking CTAB influence on  $J$ - $V$  characteristics. Both the short-circuit current density ( $J_{sc}$ ) and open-circuit voltage ( $V_{oc}$ ) of the cell fabricated with CTAB increase from 3.6 to 6.7 mA/cm<sup>2</sup> and from 0.56 to 0.61 V, respectively, relative to those of the cell prepared without using CTAB. The fill factor, however, remains nearly the same, being 0.52. As a result of these enhancements the overall energy conversion efficiency ( $\eta$ ) of the CTAB-benefited cell increases from 1.0% to 2.2%. From these values it can be easily understood that  $J_{sc}$  largely contributes to the  $\eta$  increase. The  $J_{sc}$  increase in this case of the CTAB-routed cell is in good agreement with the IPCE increase, as shown in Figure 7, where the unfailing higher IPCE of the film formed with CTAB over the visible region, compared with that without CTAB, can be seen. The higher photocurrent can be correlated with the increased surface area and the improved film morphology together with the enhanced particle crystallinity in the film formed in the presence of CTAB, compared with those obtained in the absence of CTAB. The surface area increase is attributed to a more densely packed film with smaller clusters, consisting of near-spherical TiO<sub>2</sub> particles.<sup>6</sup> An increase in surface area facilitates adsorption of a larger

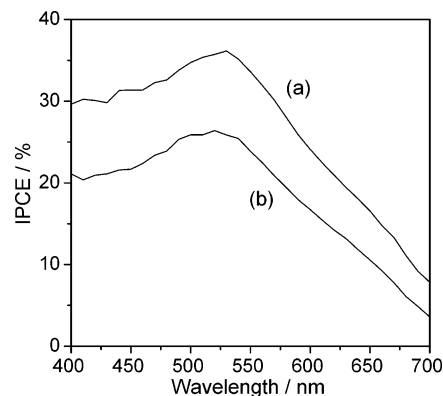


**Figure 7.** IPCE spectra of DSSCs prepared with rutile TiO<sub>2</sub> films formed (a) with and (b) without CTAB.

quantity of dye molecules, and thereby enhances the electron injection efficiency. The photocurrent increase (2.2-fold) with CTAB is disproportionately higher, taking into account the increase in dye adsorption by 35% in this case. Thus, the  $J_{sc}$  increase should have also been additionally due to the efficiency of collecting injected electrons. A higher electron-collection efficiency could result from increased interparticle electrical contact, associated with the dense packing of the particles in the film mentioned in the context of SEM analysis (Figure 1) and with increased crystallinity.<sup>8</sup>

Contrary to the enormous  $J_{sc}$  increase,  $V_{oc}$  increased by only about 50 mV in the case of the cell containing a CTAB-catalyzed TiO<sub>2</sub> film. A large surface area is expected to increase the number of surface recombination centers, leading to a  $V_{oc}$  decrease.<sup>28</sup> However, the effect of recombination on the photovoltage arising from increased surface area in this study is presumably more than offset by the decrease in back electron transfer of the conduction band electrons to triiodide ions (eq 1), due to the less open



pore structure of the CTAB-influenced film (Figure 1). In all probability, more densely interconnected TiO<sub>2</sub> particles in the CTAB-influenced film electrode create less void volume compared with that made without CTAB, causing the I<sub>3</sub><sup>-</sup> ion concentration to decrease and thus lowering the back electron transfer, as evident by the dark current decrease, shown at the bottom of Figure 6. The dark current decrease is consistent with the  $V_{oc}$  increase. The  $V_{oc}$  increase by 50 mV implies a decrease of the I<sub>3</sub><sup>-</sup> ion concentration by about 1/7, according to the equation

$$V_{oc} = (kT/e) \ln(I_{inj}/n_{cb}k_{et}[I_3^-]) \quad (2)$$

assuming that the increase of the charge flux  $I_{inj}$  from sensitized injection due to the surface area increase is approximately equal to the increase of the surface electron concentration at the TiO<sub>2</sub> surface,  $n_{cb}$ , and the rate constant of the I<sub>3</sub><sup>-</sup> reduction,  $k_{et}$ , remains essentially the same regardless of whether CTAB is present.

It is emphasized here that the photoenergy conversion efficiency is not optimized in absolute terms for film thickness, electrolyte type and concentration, and cell dimension and configuration, in view of the comparative nature of this study regarding the beneficial influence of CTAB on the enhancement of photovoltaic properties of dye-sensitized rutile TiO<sub>2</sub> solar cells. Translating the idea

(28) Schlichthörl, G.; Huang, S. Y.; Sprague, J.; Frank, A. J. *J. Phys. Chem. B* **1997**, *101*, 8141.

of the beneficial influence of the surfactant into an optimized cell can render higher efficiency in absolute terms.

On the basis of the results above, a possible role of CTAB in TiO<sub>2</sub> film formation is suggested. It is known that two types of OH groups exist on the TiO<sub>2</sub> surface:<sup>29</sup> one type bound to one Ti(IV) site (terminal OH) and the other to two such sites (bridged OH). It is essential here to mention the report by Ragai and Selim<sup>30</sup> that bridged OH groups are expected to be acidic in character, owing to their strong polarization by Ti(IV). Thus, the hydrogen atoms of bridged OH groups of titanium(IV) oxo species are exchangeable with cationic headgroups of CTAB. After such an exchange process the tail groups can combine with other tail groups, whose headgroups in turn can associate with the entangled polymeric titanium(IV) hydroxide, thereby forming larger aggregates. Aggregate formation is further facilitated by hydrophobic interaction, some sort of structure-forming interaction among nonpolar groups in water.<sup>31</sup> The observation made by Wängnerud and Jönsson regarding the tendency of an ionic surfactant–aqueous system to strive for a minimum contact area between hydrocarbon parts and water is consistent with our explanation.<sup>32</sup> The entire process leads to a rapid formation of critical masses of aggregates, heavy enough to be deposited on the substrate. This explains the faster deposition of TiO<sub>2</sub> in the presence of CTAB relative to that without CTAB. During annealing of the polymeric titanium(IV) hydroxide precipitated in the presence of CTAB, gaseous products such as CO<sub>2</sub>, NH<sub>3</sub>, and H<sub>2</sub>O can inhibit agglomeration among grains to form larger TiO<sub>2</sub> particles, resulting in the formation of smaller particles, compared with those formed in the absence of CTAB. Analogous considerations apply to SDS. The terminal OH groups can be predominantly basic and exchangeable with the anions of SDS. Triton X-100 being nonionic is not expected to replace the OH groups. Indeed, Triton X-100 has exhibited no influence on the TiO<sub>2</sub> film formation, as mentioned already. Chen et al. made a similar observation with this surfactant in their study on the stability and rheological behavior of

concentrated TiO<sub>2</sub> dispersions.<sup>33</sup> The pronounced effect of CTAB over SDS may be attributed to the degree of availability of bridged and terminal OH groups for exchange, respectively. However, an exact insight into the microenvironmental conditions during the deposition of the polymeric titanium(IV) hydroxides and their subsequent conversion into TiO<sub>2</sub> particles during annealing could not be provided at this stage.

### Conclusions

The influences of anionic SDS, nonionic Triton X-100, and cationic CTAB surfactants on the formation of a nanocrystalline rutile TiO<sub>2</sub> film from the perspective of DSSCs were investigated. While the former two categories of surfactants rendered no beneficial influence, CTAB played a significant role in improving  $J_{sc}$  and  $V_{oc}$  compared with those of the cell fabricated in its absence, thereby resulting in substantial improvement in the conversion efficiency of the pertinent cell. The increased  $J_{sc}$  is correlated with an increased amount of adsorbed dye, improved interparticle connectivity, and enhanced crystallinity of TiO<sub>2</sub> particles. The former two are associated with the particle-packing density by smaller clusters, consisting of newly observed near-spherical TiO<sub>2</sub> particles. The  $V_{oc}$  increase in the case of the CTAB-promoted cell is the combination of increased surface recombination centers due to the larger surface area and of a reduced void volume in the film, leading to a decrease in back electron transfer to triiodide ions, the latter offsetting the former. Other evidence of the beneficial effect of CTAB is faster growth of the TiO<sub>2</sub> film due primarily to the strong interaction between bridged OH groups of polymeric titanium(IV) hydroxide and cationic headgroups of CTAB, and partly to hydrophobic interaction among nonpolar groups in a water medium. Inhibition of the grain agglomeration due to the evolution of gaseous products is mentioned as the reason for obtaining smaller TiO<sub>2</sub> particle sizes in the cases of CTAB and SDS. Invariance of particle size is explained with analogous considerations.

**Acknowledgment.** This work is supported by the CRM-KOSEF, Korea University.

LA040032Q

(29) Boehm, H. P. *Discuss. Faraday Soc.* **1971**, *52*, 264.

(30) Ragai, J.; Selim, S. I. *J. Colloid Interface Sci.* **1987**, *115*, 1.

(31) Ratajczak, H.; Orville-Thomas, W. J. *Molecular Interactions*; John Wiley & Sons: New York, 1982; Vol. 3, p 285.

(32) Wängnerud, P.; Jönsson, B. *Langmuir* **1994**, *10*, 3542.

(33) Chen, X.; Cheng, H.; Ma, J. *Powder Technol.* **1998**, *99*, 171.